Electronic Supplementary Material (ESI) for Sustainable Energy & Fuels.

Co_9S_8 nanoparticles embedded in egg white-derived porous carbon as an efficient bifunctional cathode catalyst for Zn-air batteries

Weiguang Fang [a, b], Fabao Luo [a], Juanjuan Zhao [a], Huaze Dong [a], Jinmaio Zhu [a], Mingzai Wu [a, b, *]

[a] College of Chemistry and Chemical Engineering, Anhui Engineering Laboratory for Medicinal and Food Homologous Natural Resources Exploration (AEL----MFHNRE), Hefei Normal University, Hefei 230601, China

[b] Ministry of Education Key Laboratory of Structure and Functional Regulation of Hybrid Materials, Anhui University, Hefei 230601, China

1. Materials and chemicals

Eggs were purchased from local market. Cobalt nitrate hexahydrate ($Co(NO_3)_2 \cdot 6H_2O$, AR), sodium chloride (NaCl, AR), potassium hydroxide (KOH, AR), sulfur powder (AR), aqueous ammonia ($NH_3 \cdot H_2O$, AR), ethanol (AR), N,N,N',N'-tetramethylethylenediamine (AR), acrylic acid (AR) and acryl amide (AR) were all purchased from Shanghai Aladdin Chemical Reagent Co., Ltd. RuO_2, 20 wt.% Pt/C and 5% Nafion perfluorinated resin solution were purchased from Shanghai Sigma-Aldrich Chemical Reagent Co., Ltd. Deionized (DI) water was produced through twice distillations.

2. Materials characterization

The micromorphology of samples was characterized by field-emission ultra-high resolution scanning electron microscope (Hitachi Regulus 8230) and high resolution-

* Corresponding author. E-mail: wumz@ahu.edu.cn (M. Wu).

transmission electronic microscope (JEOL JEM-2100). Raman spectra, Powder X-ray diffraction (XRD) patterns and X-ray photoelectron spectroscopy (XPS) spectra were measured by in Via-Reflex confocal laser micro-Raman spectrometer (Renishaw), X-ray diffractometer with Cu K_α radiation (Rigaku smart Lab) and X-ray photoelectron spectrometer with Mg Kα achromatic X-ray source (ESCALAB 250Xi), respectively. N_2 adsorption-desorption isotherms were performed at 77 K with a specific surface and pore size analyzer (BeiShiDe 3H-2000PS2), and the special surface areas and pore size distributions were calculated by the Brunauer-Emmett-Teller (BET) method and fitted on the Barrett-Joyner-Halenda (BJH) model, respectively.

3. Electrochemical measurements

The electrochemical tests were conducted at room temperature on a Chenhua CHI 660E electrochemical work station in 0.1 M KOH solution using three electrode system which contains Ag/AgCl electrode, Pt wire and rotating disk electrode (RDE, the surface area: 0.19625 cm^2) as the reference, counter and working electrode. 10 mg of catalyst, 350 μL of deionized water, 150 μL of isopropanol, 25 μL of 5wt % Nafion solutions were mixed evenly under sonication. The working electrode was obtained after 8 μL of the obtained catalyst ink was dropped on the RDE and allowed to dry naturally. The measured potentials were calibrated to the reversible hydrogen electrode (RHE) using by using the Nernst equation ($E_{RHE} = E_{Ag/AgCl}+0.059\ pH+E^{\theta}_{Ag/AgCl}$). The cyclic voltammetry (CV) was conducted in O_2 or N_2-saturated electrolyte. The linear sweep voltammetry (LSV) was performed at a scan rate of 5 $mV \cdot s^{-1}$ in O_2-saturated electrolyte with different rotation rates from 400 to 2250 rpm. The electrochemical

impedance spectroscopy (EIS) was conducted at a bias potential of 0 V vs. Ag/AgCl with a 10 mV amplitude and in a frequency range from 1 to 100,000 Hz.

4. Preparation of solid-state hydrogel polymer electrolyte

Solid-state hydrogel polymer electrolyte used in this work was prepared by the method employed in our previous work.[1] Typically, 9 g acryl amide, 10 mL acrylic acid and 1 mL N, N-tetramethylethylenediamine were dissolved in 100 mL DI water and stirred for 1 h with N_2 bubbling. Then, the solution was poured into a mould and cured at 60 °C for 2 h. Finally, the polymer subassemblies were immersed into solution of 6 M KOH and 0.2 M $Zn(Ac)_2$ for 24 h to produce the hydrogel alkaline polymer electrolyte, which was named PAM-PAA/6M KOH.

5. Zn-air battery measurements

Home-made aqueous ZABs were assembled using purchased three-layer molds. 1 mg catalysts coated on carbon cloth were used as the cathode, Zn plate were employed as the air anode, 6 M KOH aqueous solution containing 0.2 M $Zn(Ac)_2$ was used as the electrolyte. For flexible ZABs, interdigital carbon cloth loaded with 1 mg of catalyst (air cathode) and interdigital Zn-foil (anode) were cross-arranged on a rectangular sharped PAM-PAA/6M KOH hydrogel (solid electrolyte), and all of them were wrapped in liquid silica gel with air holes. Charge and discharge LSV curves of ZABs were obtained on a Chenhua CHI 660E electrochemical work station, the charge-discharge cycling curves and galvanostatic discharge curves of ZABs were recorded by using a LAND testing system. The energy density and specific capacity of ZABs were calculated normalized to the mass of consumed Zn using the following equations,

$$Specific\ capacity = \frac{Current \times Discharge\ time}{Weight\ of\ comsumed\ Zn} \quad (1)$$

$$Energy\ density = \frac{Current \times Discharge\ time \times Average\ discharge\ voltage}{Weight\ of\ comsumed\ Zn} \quad (2)$$

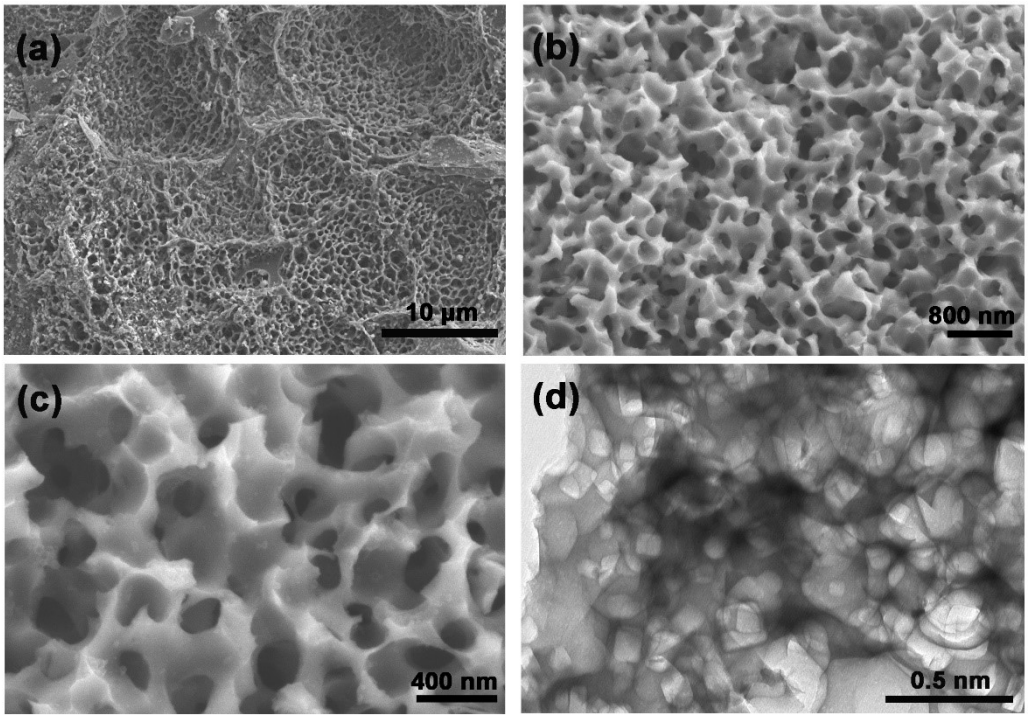

Fig. S1. (a-c) SEM and (d) TEM image of EWPC.

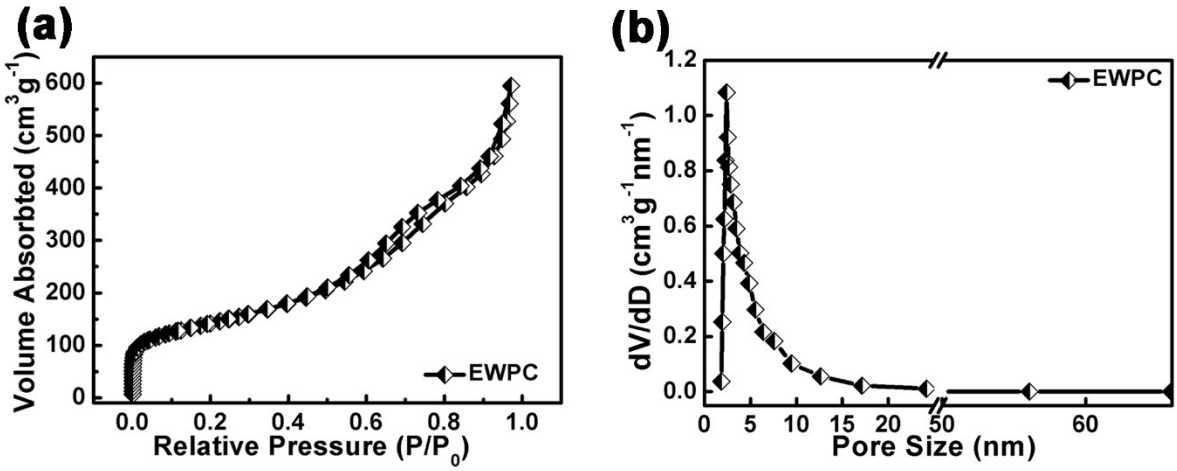

Fig. S2. (a) N_2 adsorption-desorption isotherms and (b) BJH pore-size distribution curve of EWPC.

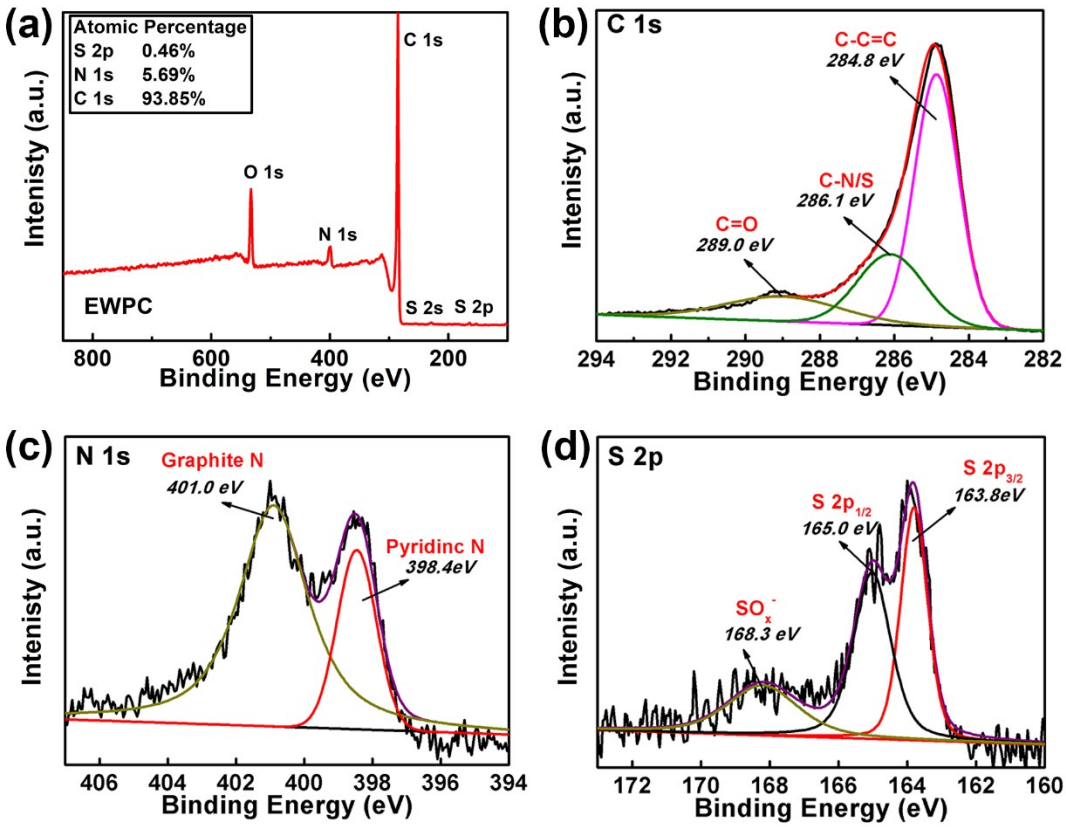

Fig. S3. (a) The survey XPS spectrum and (b-d) detailed C 1s, N 1s and S 2p XPS spectra of EWPC.

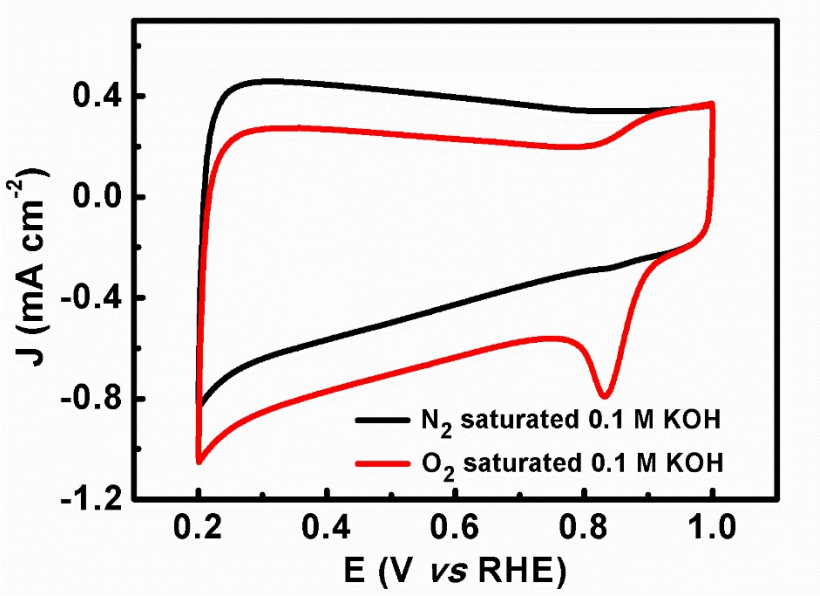

Fig. S4. CV curves of Co_9S_8/EWPC in O_2 and N_2 saturated 0.1 M KOH, respectively.

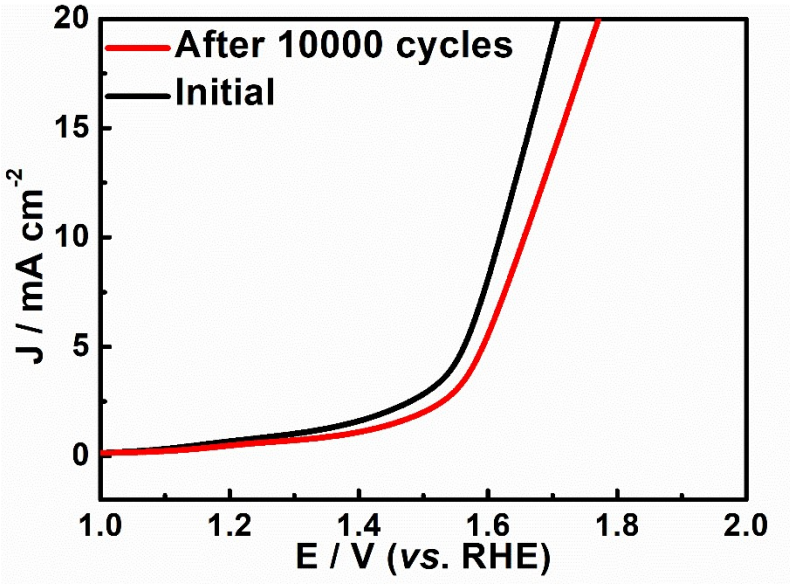

Fig. S5. OER-LSV curves of Co_9S_8/EWPC in initial and after continuous CV operation (0.2-1.0 V, 100 mV s^{-1}), respectively.

Fig. S6. The open-circuit voltage of liquid ZAB based on Pt/C + RuO_2 catalyst.

Table S1 Comparative summary of the performances of previously reported flexible ZABs with our work.

Cathode catalyst	Open-circuit voltage	Power density	Specific capacity	Cycling stability	Ref
Co_9S_8/EWPC	1.325 V	72.4 mW cm^{-2}	799.4 mAh g^{-1}	91 cycles (at 5 mA cm^{-2})	**This work**
Co@NCNTA/CC	1.484 V	38.6 mW cm^{-2}	368 mAh g^{-1}	19 h (at 1 mA cm^{-2})	[1]
$Co_{5.47}N$@N-rGO	/	54.6 mWcm^{-2}	610 mAh g^{-1}	40 h (at 1 mA cm^{-2})	[2]
CNT@POF	1.39 V	22.3 mW cm^{-2}	/	12 cycles at 1 mA cm^{-2}	[3]
IOSHs-NSC-Co_9S_8	1.408 V	60 mW cm^{-2}	738 mAh g^{-1}	105 cycles (at 5 mA cm^{-2})	[4]

S-Ni_3FeN/NSG-700	1.38 V	140.1 mW cm^{-2}	/	35 h (at 10 mA cm^{-2})	[5]
$(Ni,Co)_3O_4$@Ni-$foam_{24}$	/	73.8 mW cm^{-2}	713 mAh g^{-1}	180 cycles (at 10 mA cm^{-2})	[6]
Co/Co_3O_4/3D-NC	/	37.8 mW cm^{-2}	8.5 mAh cm^{-2}	65 cycles (at 1 mA cm^{-2})	[7]
$LaNiO_3$/NCNT	/	28.2 mW cm^{-2}	14.4 mAh	120 cycles (at 1 mA cm^{-2})	[8]
Co_3O_4/MnO_2-CNTs	1.40 V	62.5 mW cm^{-2}	~492 mAh g^{-1}	~24 cycles (at 5 mA cm-^{2})	[9]
Co_3O_4/CC	1.35 V	/	595 mA h g^{-1}	20 cycles at 2 mA cm^{-2}	[10]
ultrathin Co_3O_4/CC	1.33 V	15 mW cm^{-2}	495 mAh g-1	30 cycles (at 2 mA cm^{-2})	[11]
N-GQDs/$NiCo_2S_4$/CC	1.406 V	26.2 mW cm^{-2}	/	12 h	[12]
Fe-Co_4N@N-C	1.34 V	72.4 mW cm^{-2}	/	45 cycles (at 4 mA cm^{-2})	[13]
CMO/NCNF	1.35 V	39.3 mW cm^{-2}	/	4 h (at 1 mA cm^{-2})	[14]
$NiCo_2O_4$@NiCoFee-OH nanoarrays	1.31 V	31.8 mW cm^{-3}	/	15 h (at 2 mA cm^{-3})	[15]
$CoSe_2$-NCNT NSA	1.37 V	51.1 mW cm^{-2}	/	300 min (at 2 mA cm^{-2})	[16]
$NiCo_2NS$	1.255 V	/	/	60 cycles (at 2 mA cm^{-2})	[17]
SilkNC/KB	/	32.3 mW cm^{-2}	/	30 cycles (at 1 mA cm^{-2})	[18]

Reference

[1] Z. Cao, H. Hu, M. Wu, K. Tang, T. Jiang, *J. Mater. Chem. A*. 2019, **7**, 17581–17593.

[2] L. Liu, Y. Wang, F. Yan, C. Zhu, B. Geng, Y. Chen and S. lei Chou, *Small Methods*, 2020, **4**, 1900571.

[3] X. Shu, S. Chen, S. Chen, W. Pan and J. Zhang, *Carbon*, 2020, **157**, 234–243.

[4] B. Q. Li, S. Y. Zhang, B. Wang, Z. J. Xia, C. Tang and Q. Zhang, *Energy Environ. Sci.*, 2018, **11**, 1723–1729.

[5] K. Tang, C. Yuan, Y. Xiong, H. Hu and M. Wu, *Appl. Catal. B Environ.*, 2020, **260**, 118209.

[6] C. Lai, M. Gong, Y. Zhou, J. Fang, L. Huang, Z. Deng, X. Liu, T. Zhao, R. Lin, K. Wang, K. Jiang, H. Xin and D. Wang, *Appl. Catal. B Environ.*, 2020, **274**, 119086.

[7] N. Xu, J. A. Wilson, Y. D. Wang, T. Su, Y. Wei, J. Qiao, X. D. Zhou, Y. Zhang and S. Sun, *Appl. Catal. B Environ.*, 2020, **272**, 118953.

[8] C. Lin, S. S. Shinde, Y. Wang, Y. Sun, S. Chen, H. Zhang, X. Li and J. H. Lee, *Sustain. Energy Fuels*, 2017, **1**, 1909–1914.

[9] J. Fu, D. U. Lee, F. M. Hassan, Z. Bai, M. G. Park and Z. Chen, *Adv. Mater.*, 2015, **27**, 5617–5622.

[10] N. Xu, Y. Liu, X. Zhang, X. Li, A. Li, J. Qiao and J. Zhang, *Sci. Rep.*, 2016, **6**, 33590.
[11] S. Qu, Z. Song, J. Liu, Y. Li, Y. Kou, C. Ma, X. Han, Y. Deng, N. Zhao, W. Hu and C. Zhong, *Nano Energy*, 2017, **39**, 101–110.
[12] X. Chen, B. Liu, C. Zhong, Z. Liu, J. Liu, L. Ma, Y. Deng, X. Han, T. Wu, W. Hu and J. Lu, *Adv. Energy Mater.*, 2017, **7**, 1–11.
[13] W. Liu, B. Ren, W. Zhang, M. Zhang, G. Li, M. Xiao, J. Zhu, A. Yu, L. Ricardez-Sandoval and Z. Chen, *Small*, 2019, **15**, 1903610.
[14] Q. Xu, H. Jiang, Y. Li, D. Liang, Y. Hu and C. Li, *Appl. Catal. B Environ.*, 2019, **256**, 117893.
[15] X. Chen, Z. Yan, M. Yu, H. Sun, F. Liu, Q. Zhang, F. Cheng and J. Chen, *J. Mater. Chem. A*, 2019, **7**, 24868–24876.
[16] S. Li, X. Yang, S. Yang, Q. Gao, S. Zhang, X. Yu, Y. Fang, S. Yang and X. Cai, *J. Mater. Chem. A*, 2020, **8**, 5601–5611.
[17] W. Liu, D. Zheng, L. Zhang, R. Yin, X. Xu, W. Shi, F. Wu, X. Cao and X. Lu, *Nanoscale*, 2021, **13**, 3019–3026.
[18] L. Zhao, G. Zhang, B. Wang and G. Li, *Chem. A Eur. J.*, 2022, **28**, e202200036.
[19] C. Wang, N. H. Xie, Y. Zhang, Z. Huang, K. Xia, H. Wang, S. Guo, B. Q. Xu and Y. Zhang, *Chem. Mater.*, 2019, **31**, 1023–1029.